agronomy

MDPI

Article

Insights into the Coloring Mechanism of Dark-Red and Yellow Fruits in Sweet Cherry through Transcriptome and Metabolome Analysis

Chaoqun Chen †, Yao Zhang †, Wanjia Tang, Hongxu Chen and Ronggao Gong *

College of Horticulture, Sichuan Agricultural University, Chengdu 611130, China; 2020205005@stu.sicau.edu.cn (C.C.); 2021305052@stu.sicau.edu.cn (Y.Z.); 17843559322@163.com (W.T.); s20166113@stu.sicau.edu.cn (H.C.)

* Correspondence: gongronggao@sicau.edu.cn

† These authors contributed equally to this work.

Abstract: The color of sweet cherry fruits is an important indicator of their appearance and quality. That influences the purchasing desires of consumers. We performed a multi-omics analysis of two different colors of sweet cherry fruits (yellow "Bing Hu" and dark-red "Hong Deng" fruits). A total of 12 flavonoid differential metabolites, including hesperetin, rutin, and quercetin, and 18 differential structural genes, including *PAL*, *CHS*, *FLS*, and *DFR*, were identified. Possible key regulatory genes for the second stage of color change (from green to yellow) of "Bing Hu" sweet cherry fruits were identified as SBP, bHLH, WD40, and bZIP, which regulated the accumulation of flavonoids, including hesperetin and naringenin. In addition, the possible important roles of transcription factors, which were mainly MYB, bHLH, AP2, and WRKY, in the third stage of color change in both fruits were also identified. This study offers new insights into the changes in fruit coloration between yellow and dark-red sweet cherries, while the analysis of key metabolites and differential genes lays a molecular foundation for future color improvement and breeding programs.

Keywords: sweet cherry; flavonoids; fruit color; transcriptome; metabolome

Citation: Chen, C.; Zhang, Y.; Tang, W.; Chen, H.; Gong, R. Insights into the Coloring Mechanism of Dark-Red and Yellow Fruits in Sweet Cherry through Transcriptome and Metabolome Analysis. *Agronomy* **2023**, *13*, 2397. https://doi.org/10.3390/agronomy13092397

Academic Editors: Guanglong Wang, Lijun Ou and Aisheng Xiong

Received: 13 August 2023
Revised: 13 September 2023
Accepted: 15 September 2023
Published: 17 September 2023

1. Introduction

Plants contain various pigments, which are mainly chlorophyll, carotenoids, and anthocyanins [1]. These pigments, in turn, give plants their different colors. Plant pigments are also essential in plant growth and development and play a significant role in biological processes such as endogenous hormone synthesis and enhancement of tolerance to oxidative and drought stress [2–4]. Anthocyanins are highly safe and free of toxic side effects, as well as having good health functions, including antioxidant, antiaging, and blood pressure-lowering effects [5]. Among them, anthocyanins belong to flavonoids, which are the most widely distributed in plants. They mainly include cyanidin, delphinidin, malvidin, peonidin, petunidin, and pelargonidin. The components and proportions of anthocyanins determine the color of plant tissues. As a result, plants form different colors, such as red, purple, blue, and yellow [6].

In plants, large amounts of flavonoid compounds, such as flavones, flavonoids, and flavonols, are produced through phenylpropanoid biosynthesis, flavonoid biosynthesis, and flavone and flavonol biosynthesis [7]. In Chinese cherries, through targeted metabolism studies, Wang et al. found that the content of flavanol was much higher in yellow cherries than in red cherries [8]. Flavonoids are mainly synthesized from substances such as p-coumaroyl-CoA and cinnamoyl-CoA through various enzymatic reactions, which include the structure genes *CHI*, *CHS*, *F3H*, and *FLS* [9]. In addition, various transcription factors hold a key position in the synthesis of fruit flavonoids. The flavonoid biosynthesis pathway is transcriptionally regulated by the MBW complex formed by MYB transcription factors,

the bHLH structure, and WD40 proteins [10]. In apples, *MdMYB90-like* plays a key role in the regulation of anthocyanin biosynthesis [11]. In strawberry studies, yeast two-hybrid and BiFC assays also confirmed that the MBW complex can function in the flavonoid metabolic pathway in the form of FaMYB5/FaMYB10-FaEGL3 (bHLH)-FaLWD1/FaLWD1-like (WD40) [12]. Similar findings were also presented in *Arabidopsis thaliana* and *Norway spruce* [13,14].

The sweet cherry (*Prunus avium* L.) is a perennial fruit tree of the genus *Prunus* in the family Rosaceae that is native to the Mediterranean region of Europe and is currently one of the fastest-developing economic fruit trees [15]. The sweet cherry is a diploid (2n = 16) species composed of 16 chromosomes, and its fruit is rich in sugars, organic acids, vitamins, trace elements, and other nutrients. In addition, it contains large numbers of biologically active substances, such as anthocyanins, phenolic acids, and flavonoids, with antioxidant activity and health effects [16]. Sweet cherry fruits are colorful and glossy, and the skin and flesh show purple-black, red, yellow, and other rich fruit colors. Three stages are involved in the natural development of red sweet cherries: the green ripening stage, the color change stage, and the full red stage [17]. The fruit is green in the first stage; it changes from green to yellow in the second stage; and it changes from yellow to red in the third stage. A similar finding was found in a comparative analysis of the yellow apple mutant and its parent. In this analysis, only part of the fruit turned red while the whole remained yellow, which is probably due to the collective suppression of 34 genes related to coloration [18].

Consumers mainly prefer sweet cherries with a gaily color compared with other qualities [19]. The abundant bioactive substances in plants play an essential role in plants' growth and development but are also closely related to human health. For the last few years, research on sweet cherries has developed rapidly, and important progress has been made mainly in postharvest preservation, fruit softening, hormone treatment, and growth and developmental stages [20–23]. However, the main substances that affect the coloring of the fruit still lack certainty. Therefore, the key candidate genes and potential molecular mechanisms that regulate the accumulation of flavonoids in sweet cherry fruits of different colors need to be explored. In this experiment, we used physiological, metabolomic, and transcriptomic analyses to explore the differences in flavonoids between the yellow-colored variety of sweet cherries "Bing Hu" and the dark-red cultivar of sweet cherries "Hong Deng". The results elucidated the key differential metabolites that form fruit color during ripening of sweet cherry fruits of both colors, along with the genes associated with flavonoid formation. These results provide new insights into changes in fruit coloration in yellow and dark-red sweet cherries, while the key screened metabolites and differential genes provide a molecular basis for future color improvement and breeding programs.

2. Materials and Methods

2.1. Plant Materials

Two types of sweet cherries, including "Hong Deng" (dark red) and "Bing Hu" (yellow), whose rootstocks were *Prunus tomentosa*, were collected in the sweet cherry test base in Xixi Township and Jiuxiang Township, Hanyuan County, Ya'an City, Sichuan Province, China (longitude 102.547, latitude 29.588, altitude 1350 m). Three sweet cherry fruit trees with consistent growth conditions were selected for each variety. Fruits of uniform size, identical appearance, and without damage were selected from each orientation at the time of ripening (55 days after flowering) for sampling. The samples were returned to the laboratory immediately for photographing and then quickly cut into uniform pieces, quick-frozen with liquid nitrogen, wrapped in tin foil, and stored in the refrigerator at −80 °C. Three biological replicates were set up for each sample.

2.2. Determination of Fruit Color

2.2.1. Determination of Anthocyanin Content

Anthocyanin content was determined using the 1% hydrochloric acid–methanol method [24]. A total of 0.5 g of the sample was weighed and added to 10 mL of hy-

drochloric acid–methanol (1/99, *v*/*v*). Then, it was shaken well and placed at 4 °C to avoid light extraction overnight. Thereafter, it was ultrasonicated at 4 °C for 30 min. Next, it was centrifuged at 8000 rpm at 4 °C for 5 min. Subsequently, the absorbance was measured at 530, 620, and 650 nm. Finally, the anthocyanin content was calculated according to the formula.

$$OD\lambda = (OD530 - OD620) - 0.1\,(OD650 - OD620)$$

$$\text{Anthocyanin content (nmol/g)} = (OD\lambda/\varepsilon\lambda) \times (V/M) \times 10^6$$

where ODλ denotes the calculated optical density of anthocyanins at each wavelength; ελ denotes the molar extinction coefficient of anthocyanins, which is 4.62×10^4; V denotes the total volume of extract; and M denotes the weight of sampling.

2.2.2. Determination of Total Flavonoid Content

The total flavonoid content (TFC) was determined using the method of Wang et al. with slight modifications [25]. The extraction solution was 70% methanol containing 2% formic acid (*v*/*v*). Fruits were weighed to 0.2 g, ground, and added to 5 mL of solution and sonicated for 30 min, followed by shaking at 250 rpm for 2 h at 30 °C on a shaker to fully extract. Centrifugation was performed at 8000× *g* for 10 min, and the supernatant was removed. By using 200 µL of fruit extract, 1.3 mL of methanol, 100 µL of $NaNO_2$ (0.5 M), and 100 µL of $AlCl_3$ (0.3 M) were added sequentially and mixed in a centrifuge tube. Then, 500 µL of NaOH (1 M) was added after 5 min, and the absorbance was measured at 510 nm.

2.3. Metabolomic Analysis

Tissues (100 mg) were individually ground with liquid nitrogen, and the homogenate was resuspended in prechilled 80% methanol by vortexing. Samples were incubated on ice for 5 min and then centrifuged at 15,000× *g* and 4 °C for 20 min. Some of the supernatant was diluted to a final concentration containing 53% methanol by liquid chromatography-mass spectrometry (LC-MS). The samples were subsequently centrifuged at 15,000× *g* and 4 °C for 20 min. Finally, the supernatant was injected into the LC-MS/MS system for analysis.

Samples were injected onto a Hypesil Gold column (C18) (100 × 2.1 mm, 1.9 µm) using a 12 min linear gradient at a flow rate of 0.2 mL/min and a column temperature of 40 °C with an automatic injector set at 8 °C. The eluents for the positive polarity mode were eluent A (0.1% FA in water) and eluent B (methanol). The eluents for the negative polarity mode were eluent A (5 mM ammonium acetate, pH 9.0) and eluent B (methanol). The solvent gradient was set as follows: 2% B, 1.5 min; 2–8% B, 3 min; 85–100% B, 10 min; 100–2% B, 10.1 min; and 2% B, 12 min. The Q Exactive TM HF-X mass spectrometer was operated in positive–negative polarity mode with a spray voltage of 3.5 kV, a capillary temperature of 320 °C, a sheath gas flow rate of 35 pounds per second (psig), and positive/negative polarity mode. The aux gas flow rate was 10 L/min, the S-lens RF level was 60, and the aux gas heater temperature was 350 °C.

The raw data files generated by UHPLC-MS/MS were processed using Compound Discoverer 3.1 (CD3.1, Thermo Fisher, San Jose, CA, USA) to perform peak alignment, peak picking, and quantitation for each metabolite. Then, peaks were matched with the mzCloud (https://www.mzcloud.org/ (accessed on 16 March 2023)), mzVault, and MassList databases to obtain accurate qualitative and relative quantitative results.

These metabolites were annotated using the KEGG database (https://www.genome.jp/kegg/pathway.html (accessed on 20 March 2023)), the HMDB database (https://hmdb.ca/ (accessed on 25 March 2023)), and the LIPID MAPS database (http://www.lipidmaps.org/ (accessed on 26 March 2023)). We applied univariate analysis (*t*-test) to calculate the statistical significance (*p*-value). The metabolites with VIP > 1, *p*-value < 0.05, and fold change ≥ 2 or FC ≤ 0.5 were considered to be differential metabolites.

2.4. Transcriptome Sequencing

Total RNA was extracted using a total RNA kit (TIANGEN Biotech, Beijing, China), and the RNA integrity was assessed using the RNA Nano 6000 Assay Kit of the Bioanalyzer 2100 system (Agilent Technologies, Santa Clara, CA, USA). mRNA was purified from total RNA using poly-T oligo-attached magnetic beads. First-strand cDNA was synthesized using random hexamer primers and M-MuLV reverse transcriptase (RNase H−). Second-strand cDNA synthesis was subsequently performed using DNA Polymerase I and RNase H. The library fragments were purified with the AMPure XP system (Beckman Coulter, Beverly, MA, USA). Then, PCR was performed with Phusion High-Fidelity DNA Polymerase, Universal PCR Primers, and Index (X) Primer. Finally, PCR products were purified (using the AMPure XP system (Beckman Coulter, Inc., Brea, CA, USA)). The index-coded samples were clustered on a cBot Cluster Generation System using TruSeq PE Cluster Kit v3-cBot-HS (Illumina, San Diego, CA, USA). After cluster generation, the library preparations were sequenced on an Illumina NovaSeq platform, and 150 bp paired-end reads were generated.

Raw data (raw reads) in fastq format were first processed using fastp software v0.19.7. Reference genome and gene model annotation files were downloaded directly from the genome website. The index of the reference genome was built using Hisat2 v2.0.5, and paired-end clean reads were aligned to the reference genome using Hisat2 v2.0.5. featureCounts v1.5.0-p3 was used to count the read numbers mapped to each gene. Then, the FPKM (expected number of fragments per kilobase of transcript sequence per million base pairs sequenced) of each gene was calculated based on the length of the gene and the read count mapped to this gene.

Differential expression analysis of two groups was performed using the DESeq2 R package (1.20.0). The resulting p values were adjusted using Benjamini and Hochberg's approach for controlling the false discovery rate. Genes with an adjusted p value ≤ 0.05 found by DESeq2 were assigned as differentially expressed.

Gene ontology enrichment analysis of differentially expressed genes was implemented by the clusterProfiler R package v3.8.1. We used the clusterProfiler R package to test the statistical enrichment of differentially expressed genes in KEGG pathways.

2.5. qRT-PCR Analysis

qRT-PCR analysis was performed using a Bio-Rad CFX96TM real-time PCR system (Bio-Rad, Hercules, CA, USA) and 2× TSINGKE® Master qPCR Mix (SYBR Green I) (TSINGKE, Beijing, China). The amplification program was as follows: predenaturation at 95 °C for 30 s, denaturation at 95 °C for 5 s, and annealing at 60 °C for 30 s. The number of amplification cycles was 40, and each sample was repeated three times. The internal reference was ACTIN. Gene-specific primers were designed by Primer Premier 6, and the primer sequences are shown in Table S3. Gene expression was calculated using $2^{-\Delta\Delta Ct}$ [26].

2.6. Data Processing and Analysis

All indicators were determined after three repetitions. The data is sorted, counted, and plotted through Excel 16.54, SPSS 27, and GraphPad Prism 9, respectively.

3. Results

3.1. Analysis of Fruit Pigmentation of Two Sweet Cherry Cultivars

The sweet cherry fruits of "Hong Deng" (named H) and "Bing Hu" (named B) were selected separately to analyze the differences in fruit color. As observed from the phenotypes at ripening (Figure 1), the sweet cherry fruits of "Hong Deng" were dark red at ripening, whereas "Bing Hu" was yellow, as was the flesh coloration. We then determined the contents of total flavonoids (Figure 1A), anthocyanins (Figure 1B), and carotenoids (Figure 1C). The anthocyanin content of "Hong Deng" sweet cherry fruits in the ripening stage was high, amounting to 723.78 nmol/g FW. By contrast, the anthocyanin content of "Bing Hu" fruits was only 40.58 nmol/g FW. Similarly, the total flavonoid and carotenoid contents of "Hong Deng" sweet cherry fruits during ripening were higher than those of

"Bing Hu" sweet cherries, at 40.77 mg/mg FW and 0.46 μg/g FW, respectively. Although "Bing Hu" fruits contained flavonoids and carotenoids, the flavonoid content was much higher than the carotenoid content.

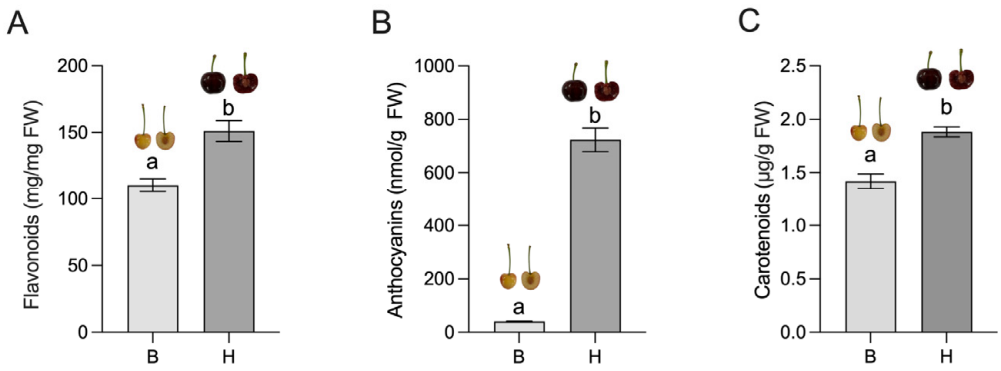

Figure 1. Differential analysis of the physiological properties of two sweet cherry fruits. (**A**) Total flavonoid content of two sweet cherry fruits at maturity; (**B**) anthocyanin content of two sweet cherry fruits at maturity; (**C**) carotenoid content of two sweet cherry fruits at maturity. Different lowercase letters indicate significant differences ($p \leq 0.05$). FW means fresh weight.

3.2. Analysis of Metabolomic Differences between Two Sweet Cherry Fruit Cultivars

A nontargeted metabolomics study was performed using LC-MS technology to investigate the metabolite variability in different color varieties of sweet cherries, and the data in positive and negative ion modes were analyzed using principal component analysis (PCA), as shown in Figure 2A. In the PCA model based on 3 quality control (QC) mix samples and 12 test samples, the first 2 principal components can be separated into 15 samples, which accounted for 57.1% and 8.6% of the total variability, respectively. In addition, two groups of test samples were separated and occupied the two ends of PC1, which indicated that sweet cherries of different colors varied greatly. A total of 532 metabolites were detected in two different varieties of sweet cherries, and the identified metabolites were annotated using the HMDB and LIPID MAPS databases. A total of 307 metabolites were categorized into 8 classes in the HMDB database (Figure 2B, Table S4), with the most abundant type being organic acids and derivatives (71 metabolites), followed by lipids and lipid-like molecules (50 metabolites), organoheterocyclic compounds (45 metabolites), and organic oxygen compounds (42 metabolites). In the LIPID MAPS database (Figure 2C, Table S5), the most abundant and diverse type was metabolism (10 classes and 305 metabolites), with amino acid metabolism and global and overview maps containing the most metabolites. Environmental Information Processing (2 classes and 14 metabolites) and Genetic Information Processing had a lesser extent. Three parameters, namely, VIP, FC, and p value (VIP > 1.0, FC > 1.5, or FC < 0.667 and p value < 0.05), were utilized to screen differential metabolites for the two varieties of sweet cherries. A total of 228 metabolites were identified as differential metabolites (150 upregulated and 78 downregulated), which indicated that most of the differential metabolites were highly abundant in the "Bing Hu" cultivars. Hierarchical cluster analysis was performed for all differential metabolites. As shown in Figure 2D, the metabolite cluster analysis of the 2 varieties showed a clear grouping pattern with good reproducibility, and all the differential metabolites were categorized into 2 groups. Group 2 metabolites were the most abundant and highly expressed in "Bing Hu" varieties, and group 1 metabolites were highly expressed in "Hong Deng" cultivars.

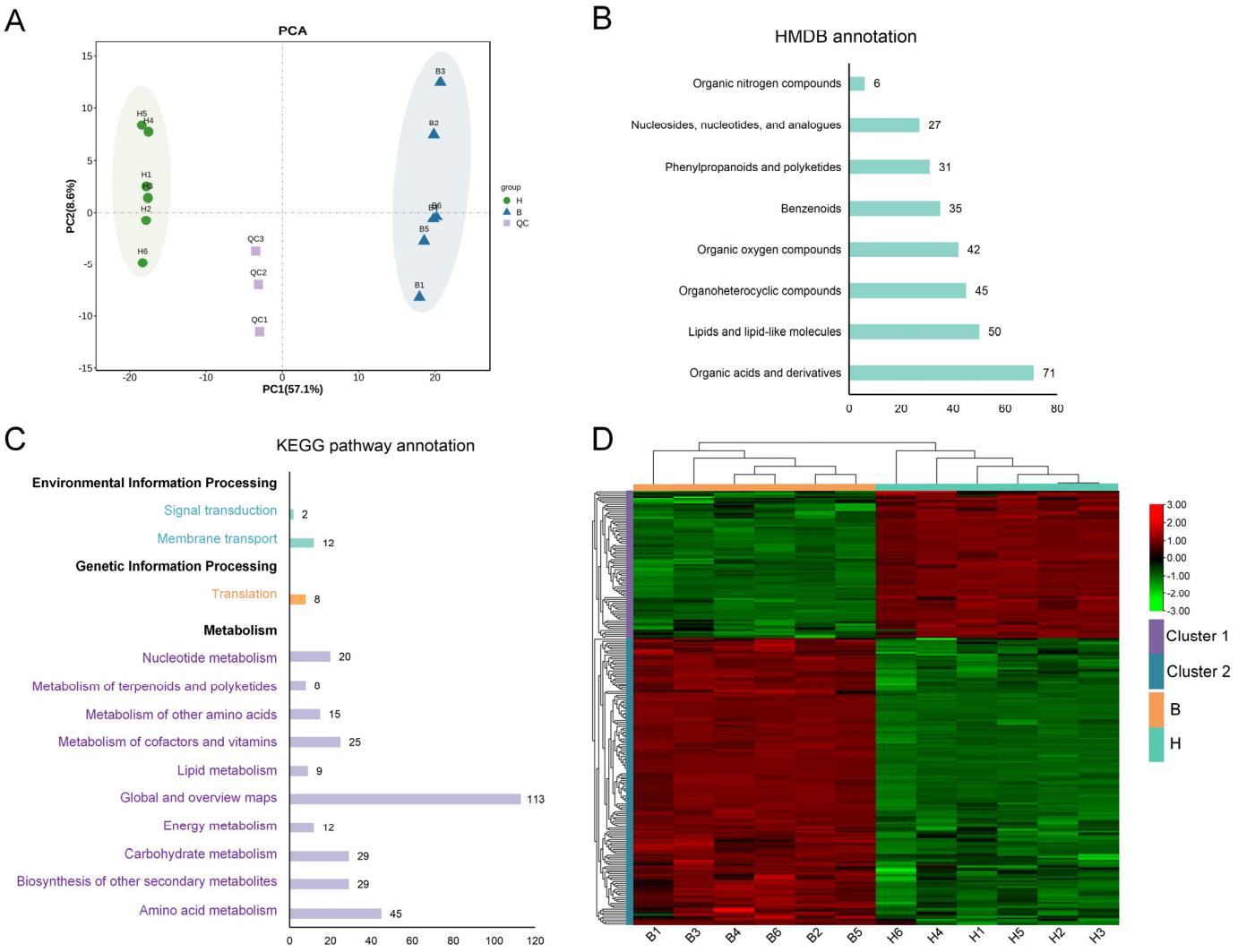

Figure 2. Metabolomic analysis of sweet cherry fruits of two cultivars. (**A**) PCA; (**B**) HMDB analysis; (**C**) KEGG pathway analysis; (**D**) Metabolite expression profile analysis.

3.3. Transcriptome Analysis of Two Cultivars of Sweet Cherry Fruits

RNA-seq technology was used to analyze the transcriptional sequencing of "Hong Deng" and "Bing Hu" sweet cherry fruits at the ripening stage. The results generated 47,709,534 raw data, and 47,119,642 high-quality clean reads were obtained after filtering out splice sequences, indeterminate reads, and low-quality reads; an average of 93.56% of the clean reads were localized to the sweet cherry genome (see Supplementary Table S1 for detailed results). A total of 44,819 transcripts were obtained, and the expression level of each gene was normalized to FPKM to get all genes' expression patterns.

The distribution of PCA among the samples is shown in Figure 3A. Among them, PC1 and PC2 accounted for 78.09% and 7.95%, respectively, and H and B were distributed at the positive and negative ends of PC1. Therefore, a large difference was observed between the two groups of previous transcripts at maturation. Meanwhile, clustering on PC1 among the three samples within each combination was high. The correlation between the samples was analyzed to further determine the repeatability between the samples, and the specific results are shown in Figure 3B. The higher correlation between the samples within each combination and the weaker correlation between the combinations further indicated that a large difference existed between the transcript levels of the sweet cherry fruit of the two cultivars.

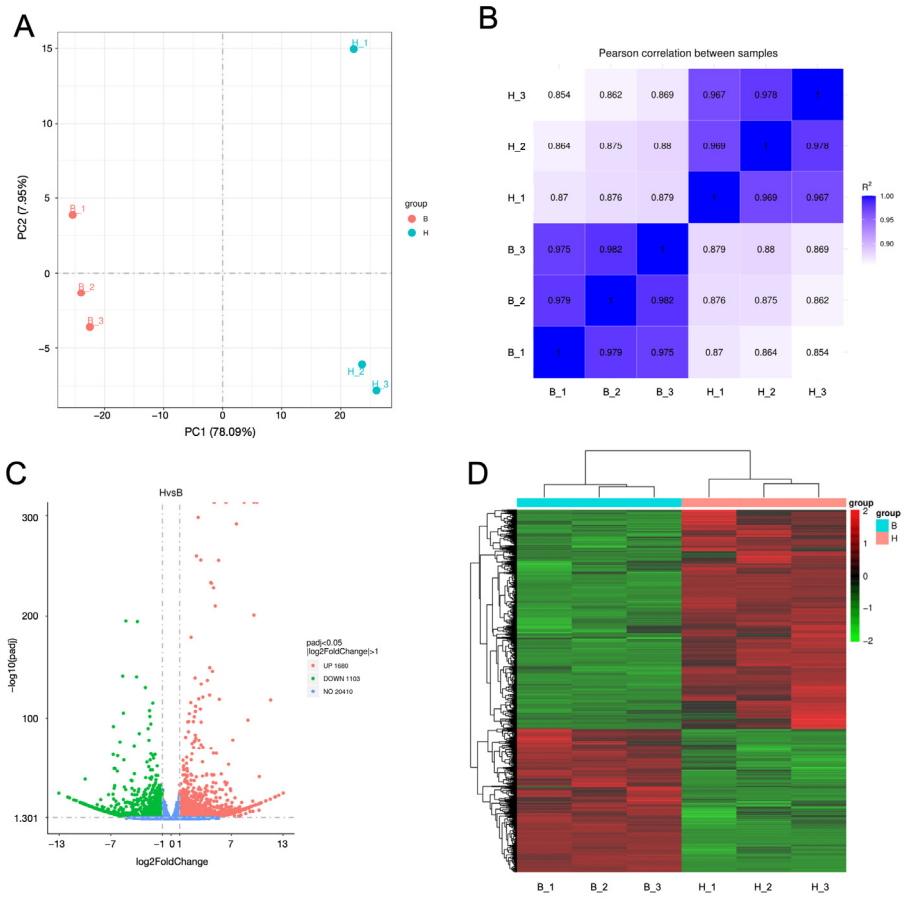

Figure 3. Transcriptome analysis of two cultivars of sweet cherry fruits. (**A**) PCA of two cultivars of sweet cherry fruits; (**B**) sample correlation analysis; (**C**) volcano plot analysis; (**D**) expression patterns of differential genes.

Using the criterion of $|\log2(\text{FoldChange})| \geq 1$ and padj ≤ 0.05 for differential gene screening, 2783 differential genes were identified, of which 1680 genes were upregulated and 1103 genes were downregulated (Figure 3C). The expression patterns of all differential genes are shown in Figure 3D. As shown in the figure, large differences were observed in the expression of these differential genes, and most of them were mainly expressed at higher levels in "Hong Deng" sweet cherries. The differential expression of these genes might be the main reason for the large differences in the fruits of the two cultivars of sweet cherries.

3.4. Multi-Omics Analysis

3.4.1. KEGG Pathway Map Analysis

A KEGG pathway analysis was performed to further identify the pathways of differential metabolites and differential gene enrichment. As shown in Figure 4A, the flavone and flavonol biosynthesis pathway was the most significant and contained three differential metabolites as plotted against $-\log10(p\text{-value})$. We also noted that the flavonoid biosynthesis, phenylpropanoid biosynthesis, and isoflavonoid biosynthesis pathways were all significantly enriched in the top 20, which suggests that flavonoids differed significantly between dark-red and yellow varieties. Similarly, the analysis of transcriptome-enriched pathways was conducted using $-\log10(\text{padj})$ (Figure 4B). As observed from the figure, flavonoid biosynthesis was not only the most prominent pathway but also contained a large number of differential genes. Meanwhile, the phenylpropanoid biosynthesis pathway contained 33 differential genes and was the second most significantly enriched pathway. All these results indicate large differences in flavonoids between dark-red and yellow cultivars.

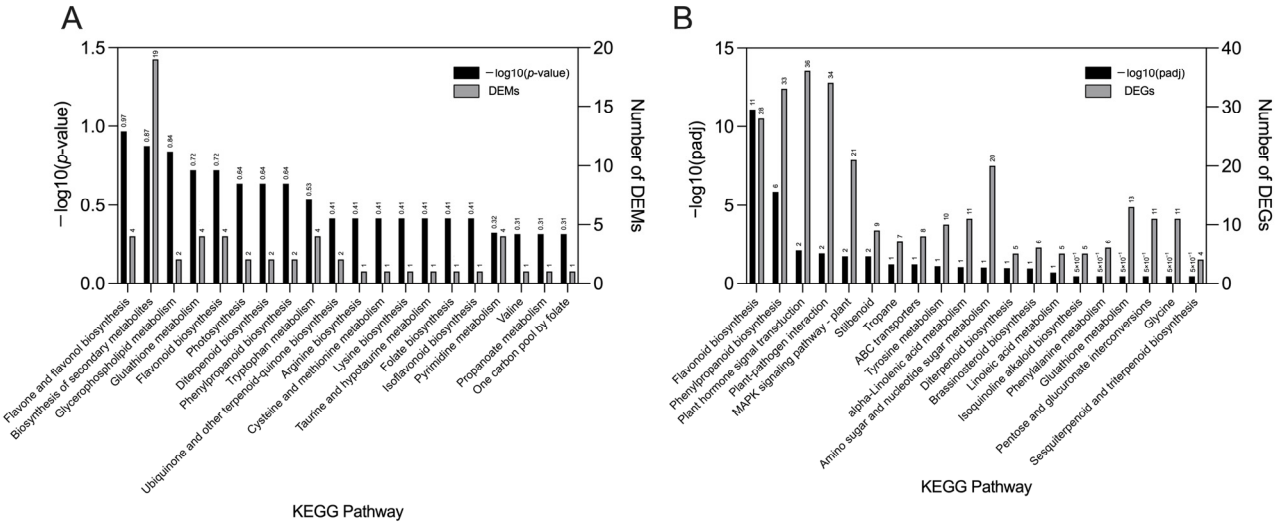

Figure 4. Annotation analysis of KEGG pathways in two sweet cherry fruit cultivars at the ripening stage. (**A**) Fruit differential metabolite KEGG pathway enrichment analysis of two cultivars as statistically mapped according to −log10(*p*-value). (**B**) Fruit differential gene KEGG pathway enrichment analysis of two cultivars as statistically mapped according to −log10(padj).

3.4.2. Flavonoid Anabolic Network Analysis

In a previous study, flavonoid-related pathways were found to be significantly enriched in the two cultivars of sweet cherry fruits; therefore, we further mapped the specific metabolic pathways (Figure 5 and Table S2). As shown in the figure, most of the flavonoids differed significantly between the two varieties of fruit. Among them, five substances, namely hesperetin, caffeic acid, ferulic acid, naringenin, and kaempferitrin, were higher in the yellow variety fruits than in the dark-red sweet cherry fruits. In addition, the remaining seven substances (luteolin, rutin, quercetin, eriodictyol, glycitein 7-O-glucoside, trifolin, and catechin) were all found at higher levels in dark-red fruit. We also analyzed the relevant differential genes in this pathway to further determine the regulatory mechanism of these substance changes. We identified a total of 18 differential genes, including E4.3.1.24 (PAL), EC: 2.3.1.74 (CHS), EC:1.14.20.6 (FLS), and EC: 1.1.1.219 (DFR). The expression of these genes was higher in dark-red fruits than in yellow varieties.

3.5. Transcription Factor Analysis

Their transcription factors were analyzed and identified, and the results are shown in Figure 6A. A total of 20 gene families with 780 genes, such as MYB, AP2, and bHLH, were identified, and the families with the most genes were MYB, AP2, FAR1, and bHLH. Among them, genes such as WRKY, which is related to plant resistance, were highly enriched. We further counted and analyzed the number of differential genes in each group of transcription factors and the expression pattern of differential transcription factors. The results are shown in Figure 6B,C. A total of 64 genes in 12 gene families were screened as differential transcription factors, and more differential genes and higher expression of the gene families of WRKY, AP2, bHLH, and MYB were related to flavonoid metabolism, among which the genes of the WRKY family were the most abundant (17, 26.56%). Most of the differential transcription factors scored higher expression in dark-red cultivars than in yellow cherries, and these differential transcription factors may be potential factors that regulate the existence of differences in fruit coloration between the two cultivars.

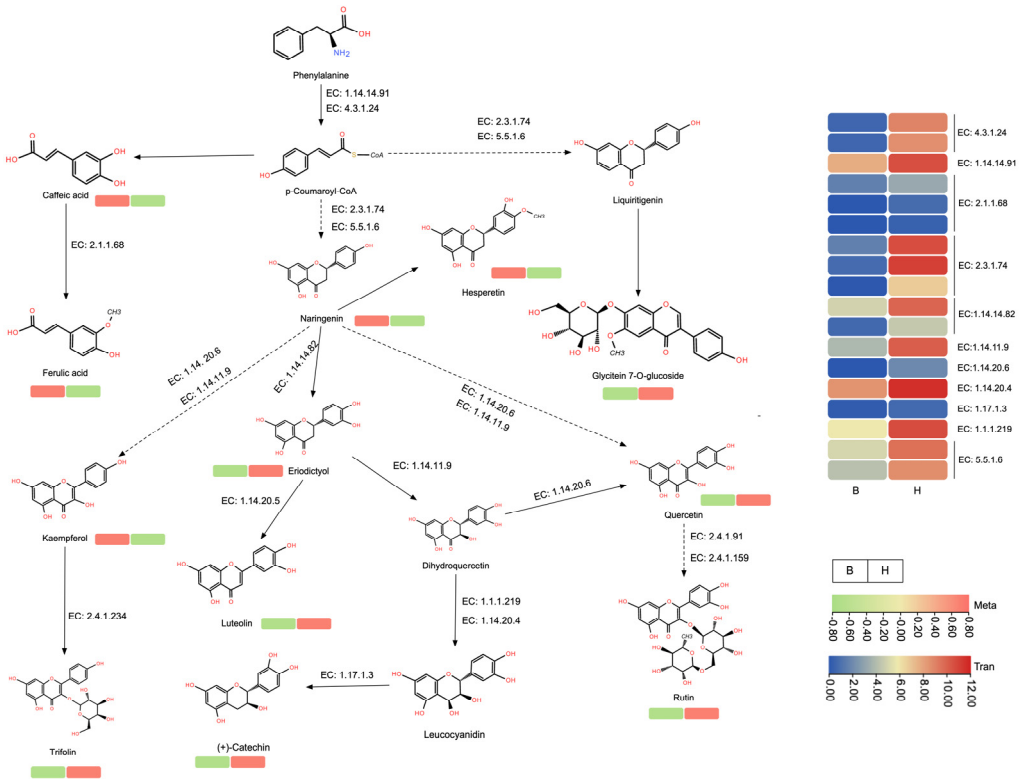

Figure 5. Flavonoid anabolic network analysis.

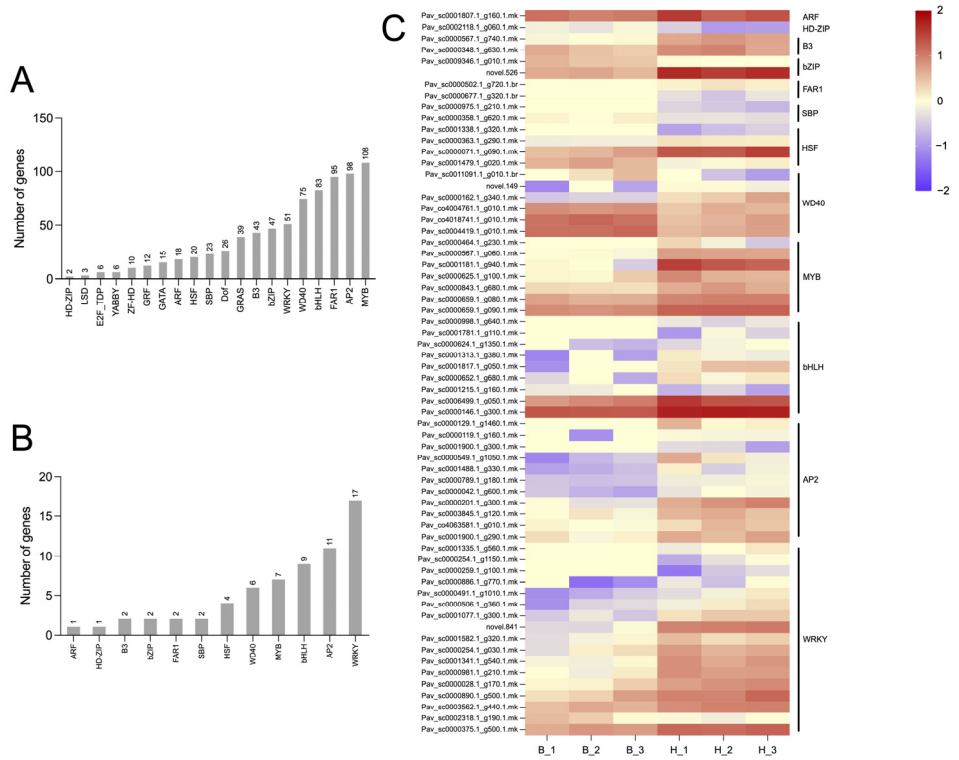

Figure 6. Transcription factor analysis of sweet cherry fruits from two cultivars. (**A**) Results of transcription factor analysis in the transcriptome; (**B**) statistics and analysis of differential transcription factors; (**C**) heatmap of the expression patterns of differential transcription factors as transformed to FPKM values of transcription factors according to log10.

3.6. Correlation Matrix Analysis

The key differential genes and transcription factors in the pathway were then analyzed in a correlation matrix. The results are shown in Figure 7. As shown in the figure, a positive correlation was observed between these transcription factors and the differential genes, except for hesperetin, caffeic acid, ferulic acid, naringenin, and kaempferitrin. In particular, some of the transcription factors boxed using black lines showed highly significant positive correlations between these differential genes and differential metabolites, which were mainly the four family genes MYB, bHLH, AP2, and WRKY. These transcription factors were more associated with fruit anthocyanin synthesis. Some transcription factors marked with red lines (mainly SBP, bHLH, WD40, and bZIP) showed high and highly significant correlations with several metabolites with higher content in yellow cultivars, which suggested that these transcription factors may be the key regulators in regulating the accumulation of flavonoids in the fruits of yellow cultivars of sweet cherries.

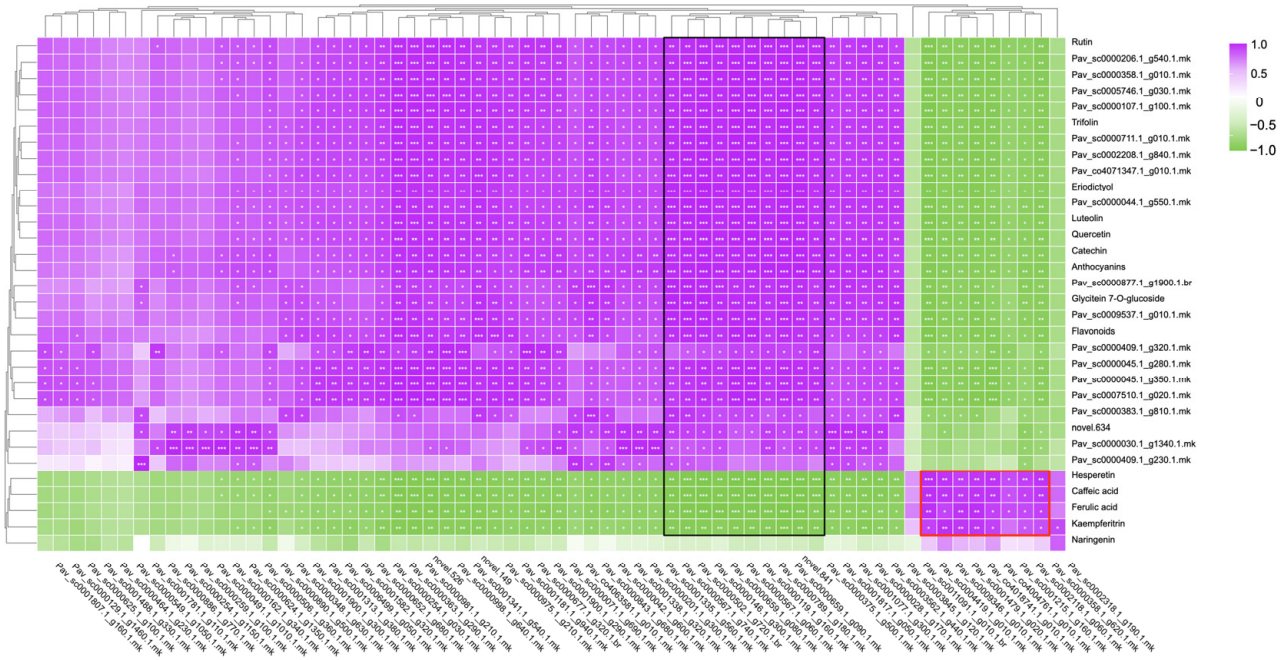

Figure 7. Correlation matrix analysis. * indicates a significant correlation at the 0.05 level; ** indicates a significant correlation at the 0.01 level; and *** indicates a highly significant correlation at the 0.001 level.

3.7. qPCR Validation Analysis

Key regulatory genes and transcription factors were randomly selected from the pathway and analyzed by qRT-PCR to verify the validity of the transcriptome, and the results are shown in Figure 8. Consistent with the transcriptome results (Table S3), most of these key structural genes were highly expressed in "Hong Deng" sweet cherries. Overall, the qRT-PCR results of most of the structural genes and transcription factors were consistent with the transcriptome data, which indicates that the transcriptome data had high confidence.

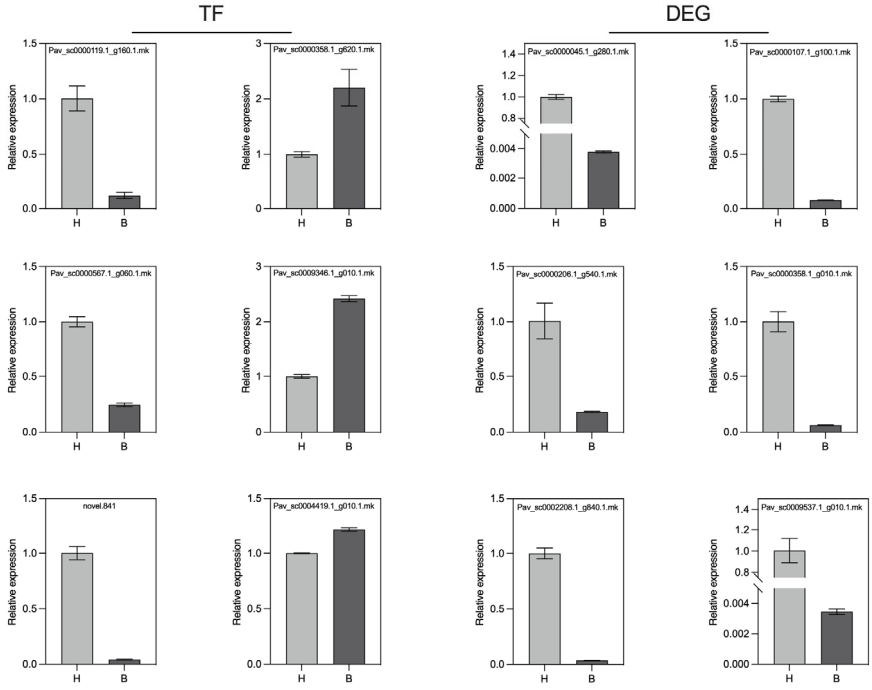

Figure 8. qRT-PCR analysis of genes and transcription factors related to flavonoid synthesis in different varieties of sweet cherry fruit.

4. Discussion

Flavonoids are a class of biologically active compounds that are beneficial to human health and are widely found in various fruits and vegetables [27–30]. Several epidemiological studies have shown that flavonoids play an important role in antioxidation, improvement of human immunity, prevention of urinary stones, treatment of hypertension, and prevention of cardiovascular diseases [31–35]. Color differences often exist between different cultivars of the same species, and flavonoids are an important source of yellow color in plants. In two differently colored cucumber cultivars, namely, L19 and L14, L14 with a yellow rind had a significantly higher flavonoid content than L19 with a green-white rind at late fruit ripening. Moreover, the carotenoid content was insignificantly different between the two cultivars [36]. Similar findings also occurred in paeonia, melon, and mulberry [37–39]. In this study, the plant source of yellow pigments (carotenoids) was much lower than the flavonoids in the "Bing Hu" fruit. Therefore, flavonoids may be the main source of substances responsible for the yellow coloration of "Bing Hu" sweet cherry fruits [40]. Therefore, flavonoids may be the main source of substances responsible for the yellow coloration of "Bing Hu" sweet cherry fruits.

The results of Metabolome showed that the pathways related to flavonoids were significantly enriched in the fruit of both sweet cherry cultivars. A total of 12 differential metabolites in the flavonoid pathway, including hesperetin, caffeic acid, luteolin, rutin, and quercetin, were identified (Table S3). Five substances (hesperetin, caffeic acid, ferulic acid, naringenin, and kaempferitrin) were higher in the yellow cultivar fruits than in the dark-red sweet cherry fruits. The remaining seven substances (luteolin, rutin, quercetin, eriodictyol, glycitein 7-O-glucoside, trifolin, and catechin) were more abundant in dark-red fruit.

Previous studies have shown that naringenin and hesperetin are two of the main substances responsible for the color differences in *Sorghum* bicolor seeds [41]. In a study of peach gum, high levels of hesperetin, naringenin, and eriodictyol were also significantly positively correlated with the deeper yellow coloration of *Sorghum* bicolor [42]. We hypothesized that higher levels of the five flavonoid metabolites, especially hesperetin and naringenin, in the yellow cultivar might be the primary reason for the yellow coloration of "Bing Hu" sweet cherry fruit. In another study on the coloration mechanism of *Cymbidium* sinense "Red Sun" leaves, the total phenol, total anthocyanin, and carotenoid contents of

yellow leaves were significantly lower than those of red leaves, which is consistent with the results of the present study [43]. In our study, luteolin, rutin, quercetin, eriodictyol, glycitein 7-O-glucoside, trifolin, and catechin, which are seven differential flavonoid metabolites that are more abundant in the dark-red cultivar, may be the main reason for making the total flavonoid content higher in the dark-red sweet cherry cultivar. However, due to the extremely high anthocyanin content in the dark-red sweet cherry cultivar, the fruit color is still dark red.

In the analysis of the flavonoid pathway, we also identified 18 differential structural genes, including *PAL*, *CHS*, *CHI*, *FLS*, *ANS*, and *DFR*, and the expression of these genes was higher in the dark-red cultivar than in the yellow cultivar. These structural genes are extensively involved in the synthesis and metabolism of flavonoids and are responsible for the higher flavonoid content in dark red fruits [7]. In addition to structural genes, plant color formation is also regulated by transcription factors [44]. Further transcription factor analysis of the fruits of the two differently colored cultivars identified 64 genes in 12 gene families as differential transcription factors. The correlation matrix showed that these transcription factors were positively correlated with the differential genes. The seven flavonoid metabolites that were more abundant in the red sweet cherry varieties. In particular, the four families of genes, MYB, bHLH, AP2, and WRKY, were significantly positively correlated with some of the differential genes (PAL, C4H, F3′H, LDOX, DFR, CHI) and metabolites (Rutin, Trifolin, Luteolin, Quercetin, Catechin, and Anthocyanins). MYB and bHLH are two important transcriptional proteins in plants, and they have regulatory roles in anthocyanin biosynthesis in fruits such as apples [45,46], strawberries [12,47], and grapes [48,49]. They are usually involved in the regulation of color accumulation in plants through the MBW ternary complex with WD40 proteins [50]. AP2 and WRKY transcription factors primarily play a role in the response of plants to abiotic stresses [51,52]. In recent years, however, they have been found to also be involved in the anthocyanin biosynthesis of plants [53,54]. In the results of this experimental study, the four families of genes showed highly significant positive correlations with seven flavonoid metabolites and differentially structured genes that were more abundant in dark-red sweet cherry cultivars. The four classes of MYB, bHLH, AP2, and WRKY transcription factors identified in our study may therefore be the major regulatory genes that lead to the high anthocyanin and flavonoid contents in dark-red sweet cherry cultivars.

In addition, we found that several metabolites (hesperetin, caffeic acid, ferulic acid, naringenin, and kaempferitrin) that were more abundant in the yellow sweet cherry cultivar were correlated with transcription factors, including SBP, bHLH, WD40, and bZIP, at higher and highly significant levels. Previous studies have shown that SBP transcription factors can be mediated by MIR156a to inhibit isoflavone biosynthesis in *Pueraria thomsonii* Benth [55]. Given that the flavonoid pathway is the upstream pathway of anthocyanin biosynthesis, bHLH and WD40, which play important roles in anthocyanin biosynthesis, also regulate the biosynthesis of flavonoids. For instance, bHLH is involved in flavonoid biosynthesis in bryophytes [56]. In a study of *Oroxylum indicum*, transcription factor analysis showed that the bHLH structure and the WD40 transcription factor family regulated the abundance of flavonoid biosynthesis [57]. In another related study, after the authors knocked out one allele of *VvbZIP36*, the amount of naringenin in grapefruit increased [58]. All these studies indicate that SBP, bHLH, WD40, and bZIP have important roles in plant flavonoid biosynthesis. On the basis of the results of this experiment, we hypothesize that these transcription factors may also be key regulators of the yellow coloration of "Bing Hu" sweet cherry fruits and the accumulation of flavonoids such as hesperetin and naringenin.

Three stages are involved in the natural development of the "Hong Deng" sweet cherry, in which the fruit changes from green to yellow and finally to red [17], while the "Bing Hu" sweet cherry only changes color from green to yellow (Figure 1). Similarly, the "Bing Hu" sweet cherry changed from green to yellow during the second stage. However, only part of the fruit peel changed color during the process of changing from yellow to red, and the main peel and flesh of the fruit were still yellow. In the study of El-Sharkawy et al.,

it was shown that fruit will not turn color when coloring-related genes are repressed [18]. Activation of genes functioning in the later stages of the pathway leading to anthocyanin (pigmentation) production (*DFR*, *LDOX*, and *UFGT)* requires the MBW complex, and flavone/isoflavone and anthocyanins compete for the same precursor substances, which are the flavanones, to determine fruit coloration. We therefore deduced that SBP, bHLH, WD40, and bZIP might be the key regulatory genes for the change from green to yellow in the second stage of "Bing Hu" sweet cherry fruit. In the third stage, during the process of yellow sweet cherry fruit changing from yellow to red, transcription factors such as MYB, bHLH, AP2, and WRKY might be suppressed. We speculated that the structural genes failed to be activated, which led to the inhibition of anthocyanin accumulation and then led to the color change of only some of the peel of the yellow sweet cherry fruits. The remaining part of the peel and flesh failed to change color to red. In the "Hong Deng" sweet cherry, the aforementioned genes were expressed, and anthocyanins accumulated, which resulted in the dark-red color of the fruit.

5. Conclusions

We determined the pigmentation differences between two different cultivars of sweet cherry, namely, "Hong Deng" and "Bing Hu," through phenotypic observation and physiological index analysis. A total of 12 flavonoid differential metabolites, including hesperetin, rutin, and quercetin, and 18 differential structural genes, including *PAL*, *CHS*, *FLS*, and *DFR*, were identified in the two sweet cherry fruits by the combination of transcriptome and metabolome analyses. Transcription factor and correlation matrix analyses indicated that the transcription factors SBP, bHLH, WD40, and bZIP might be the key regulatory genes for the second stage of yellow sweet cherry fruits changing from green to yellow color, which regulates the accumulation of flavonoids such as hesperetin and naringenin. The transcription factors MYB, bHLH, AP2, and WRKY might function in the third stage of the fruit change from yellow to red. They were repressed in yellow sweet cherry fruit and normally expressed in the dark-red sweet cherry fruit cultivar, which in turn led to the final color difference between the two sweet cherry cultivars. These results provide new insights into the changes in fruit coloration in yellow and dark-red sweet cherries, while the key screened metabolites and differential genes provide a molecular basis for future color improvement and breeding programs.

Supplementary Materials: The following supporting information can be downloaded at: https://www.mdpi.com/article/10.3390/agronomy13092397/s1, Table S1: Transcriptome sequencing statistics; Table S2: Expression of DEMs and DEGs; Table S3: Primer sequences used for qPCR. Table S4: Classification results of the HMDB database. Table S5: Classification results from the KEGG database.

Author Contributions: C.C. and Y.Z.: designed the whole experiments. C.C., W.T. and Y.Z.: Data determination. Y.Z., C.C., W.T., H.C. and R.G.: analyzed the data. C.C. and Y.Z.: wrote the manuscript. R.G.: supervision. All authors have read and agreed to the published version of the manuscript.

Funding: This research was funded by the Sichuan Science and Technology Plan Project (Key R&D Project) (2021YFN0081, 2021YFN0082).

Institutional Review Board Statement: Not applicable.

Informed Consent Statement: Not applicable.

Data Availability Statement: The data presented in this study are available upon request from the corresponding author.

Conflicts of Interest: The authors declare no conflict of interest.

Sample Availability: The data is available from the authors.

References

1. Tanaka, Y.; Sasaki, N.; Ohmiya, A. Biosynthesis of plant pigments: Anthocyanins, betalains and carotenoids. *Plant J.* **2008**, *54*, 733–749. [CrossRef] [PubMed]
2. Kadomura-Ishikawa, Y.; Miyawaki, K.; Takahashi, A.; Masuda, T.; Noji, S. Light and abscisic acid independently regulated FaMYB10 in Fragaria × ananassa fruit. *Planta* **2015**, *241*, 953–965. [CrossRef] [PubMed]
3. Lee, S.G.; Vance, T.M.; Nam, T.G.; Kim, D.O.; Koo, S.I.; Chun, O.K. Contribution of Anthocyanin Composition to Total Antioxidant Capacity of Berries. *Plant Foods Hum. Nutr.* **2015**, *70*, 427–432. [CrossRef] [PubMed]
4. Cirillo, V.; D'Amelia, V.; Esposito, M.; Amitrano, C.; Carillo, P.; Carputo, D.; Maggio, A. Anthocyanins are Key Regulators of Drought Stress Tolerance in Tobacco. *Biology* **2021**, *10*, 139. [CrossRef]
5. Lu, W.; Shi, Y.; Wang, R.; Su, D.; Tang, M.; Liu, Y.; Li, Z. Antioxidant Activity and Healthy Benefits of Natural Pigments in Fruits: A Review. *Int. J. Mol. Sci.* **2021**, *22*, 4945. [CrossRef]
6. Saigo, T.; Wang, T.; Watanabe, M.; Tohge, T. Diversity of anthocyanin and proanthocyanin biosynthesis in land plants. *Curr. Opin. Plant Biol.* **2020**, *55*, 93–99. [CrossRef]
7. Falcone Ferreyra, M.L.; Rius, S.P.; Casati, P. Flavonoids: Biosynthesis, biological functions, and biotechnological applications. *Front. Plant Sci.* **2012**, *3*, 222. [CrossRef]
8. Wang, Y.; Wang, Z.; Zhang, J.; Liu, Z.; Wang, H.; Tu, H.; Zhou, J.; Luo, X.; Chen, Q.; He, W.; et al. Integrated Transcriptome and Metabolome Analyses Provide Insights into the Coloring Mechanism of Dark-red Yellow Fruits in Chinese Cherry [*Cerasus pseudocerasus* (Lindl), G. Don]. *Int. J. Mol. Sci.* **2023**, *24*, 3471. [CrossRef]
9. Liu, W.; Feng, Y.; Yu, S.; Fan, Z.; Li, X.; Li, J.; Yin, H. The Flavonoid Biosynthesis Network in Plants. *Int. J. Mol. Sci.* **2021**, *22*, 12824. [CrossRef]
10. Gonzali, S.; Perata, P. Fruit colour and novel mechanisms of genetic regulation of pigment production in tomato fruits. *Horticulturae* **2021**, *7*, 259. [CrossRef]
11. Sun, C.; Wang, C.; Zhang, W.; Liu, S.; Wang, W.; Yu, X.; Song, T.; Yu, M.; Yu, W.; Qu, S. The R2R3-type MYB transcription factor MdMYB90-like is responsible for the enhanced skin color of an apple bud sport mutant. *Hortic. Res.* **2021**, *8*, 156. [CrossRef] [PubMed]
12. Yue, M.; Jiang, L.; Zhang, N.; Zhang, L.; Liu, Y.; Lin, Y.; Zhang, Y.; Luo, Y.; Zhang, Y.; Wang, Y.; et al. Regulation of flavonoids in strawberry fruits by FaMYB5/FaMYB10 dominated MYB-bHLH-WD40 ternary complexes. *Front. Plant Sci.* **2023**, *14*, 1145670. [CrossRef] [PubMed]
13. Baudry, A.; Caboche, M.; Lepiniec, L. TT8 controls its own expression in a feedback regulation involving TTG1 and homologous MYB and bHLH factors, allowing a strong and cell-specific accumulation of flavonoids in Arabidopsis thaliana. *Plant J.* **2006**, *46*, 768–779. [CrossRef] [PubMed]
14. Nemesio-Gorriz, M.; Blair, P.B.; Dalman, K.; Hammerbacher, A.; Arnerup, J.; Stenlid, J.; Mukhtar, S.M.; Elfstrand, M. Identification of Norway Spruce MYB-bHLH-WDR Transcription Factor Complex Members Linked to Regulation of the Flavonoid Pathway. *Front. Plant Sci.* **2017**, *8*, 305. [CrossRef]
15. Yamamoto, T.; Terakami, S. Genomics of pear and other Rosaceae fruit trees. *Breed. Sci.* **2016**, *66*, 148–159. [CrossRef]
16. Chockchaisawasdee, S.; Golding, J.B.; Vuong, Q.V.; Papoutsis, K.; Stathopoulos, C.E. Sweet cherry: Composition, postharvest preservation, processing and trends for its future use. *Trends Food Sci. Technol.* **2016**, *55*, 72–83. [CrossRef]
17. Chen, C.; Chen, H.; Yang, W.; Li, J.; Tang, W.; Gong, R. Transcriptomic and Metabolomic Analysis of Quality Changes during Sweet Cherry Fruit Development and Mining of Related Genes. *Int. J. Mol. Sci.* **2022**, *23*, 7402. [CrossRef]
18. El-Sharkawy, I.; Liang, D.; Xu, K. Transcriptome analysis of an apple (Malus × domestica) yellow fruit somatic mutation identifies a gene network module highly associated with anthocyanin and epigenetic regulation. *J. Exp. Bot.* **2015**, *66*, 7359–7376. [CrossRef]
19. Correia, S.; Queirós, F.; Ribeiro, C.; Vilela, A.; Aires, A.; Barros, A.I.; Schouten, R.; Silva, A.P.; Gonçalves, B. Effects of calcium and growth regulators on sweet cherry (*Prunus avium* L.) quality and sensory attributes at harvest. *Sci. Hortic.* **2019**, *248*, 231–240. [CrossRef]
20. Karagiannis, E.; Michailidis, M.; Karamanoli, K.; Lazaridou, A.; Minas, I.S.; Molassiotis, A. Postharvest responses of sweet cherry fruit and stem tissues revealed by metabolomic profiling. *Plant Physiol. Biochem.* **2018**, *127*, 478–484. [CrossRef]
21. Zhai, Z.; Xiao, Y.; Wang, Y.; Sun, Y.; Peng, X.; Feng, C.; Zhang, X.; Du, B.; Zhou, X.; Wang, C.; et al. Abscisic acid-responsive transcription factors PavDof2/6/15 mediate fruit softening in sweet cherry. *Plant Physiol.* **2022**, *190*, 2501–2518. [CrossRef] [PubMed]
22. Chen, C.; Chen, H.; Chen, Y.; Yang, W.; Li, M.; Sun, B.; Song, H.; Tang, W.; Zhang, Y.; Gong, R. Joint metabolome and transcriptome analysis of the effects of exogenous GA3 on endogenous hormones in sweet cherry and mining of potential regulatory genes. *Front. Plant Sci.* **2022**, *13*, 1041068. [CrossRef]
23. Michailidis, M.; Karagiannis, E.; Tanou, G.; Samiotaki, M.; Sarrou, E.; Karamanoli, K.; Lazaridou, A.; Martens, S.; Molassiotis, A. Proteomic and metabolic analysis reveals novel sweet cherry fruit development regulatory points influenced by girdling. *Plant Physiol. Biochem.* **2020**, *149*, 233–244. [CrossRef] [PubMed]
24. Li, M.; Cheng, S.; Wang, Y.; Dong, Y. Improving Fruit Coloration, Quality Attributes, and Phenolics Content in 'Rainier' and 'Bing' Cherries by Gibberellic Acid Combined with Homobrassinolide. *J. Plant Growth Regul.* **2020**, *39*, 1130–1139. [CrossRef]
25. Wang, X.; Li, C.; Liang, D.; Zou, Y.; Li, P.; Ma, F. Phenolic compounds and antioxidant activity in red-fleshed apples. *J. Funct. Foods* **2015**, *18*, 1086–1094. [CrossRef]

26. Livak, K.J.; Schmittgen, T.D. Analysis of relative gene expression data using real-time quantitative PCR and the 2(-Delta Delta C(T)) Method. *Methods* **2001**, *25*, 402–408. [CrossRef]
27. Zhao, C.; Wang, F.; Lian, Y.; Xiao, H.; Zheng, J. Biosynthesis of citrus flavonoids and their health effects. *Crit. Rev. Food Sci. Nutr.* **2020**, *60*, 566–583. [CrossRef] [PubMed]
28. Nassiri-Asl, M.; Hosseinzadeh, H. Review of the Pharmacological Effects of *Vitis vinifera* (Grape) and its Bioactive Constituents: An Update. *Phytother. Res.* **2016**, *30*, 1392–1403. [CrossRef]
29. Jia, X.; Xie, H.; Jiang, Y.; Wei, X. Flavonoids isolated from the fresh sweet fruit of Averrhoa carambola, commonly known as star fruit. *Phytochemistry* **2018**, *153*, 156–162. [CrossRef]
30. Wu, M.; Xu, X.; Hu, X.; Liu, Y.; Cao, H.; Chan, H.; Gong, Z.; Yuan, Y.; Luo, Y.; Feng, B.; et al. SlMYB72 Regulates the Metabolism of Chlorophylls, Carotenoids, and Flavonoids in Tomato Fruit. *Plant Physiol.* **2020**, *183*, 854–868. [CrossRef]
31. Kozłowska, A.; Szostak-Wegierek, D. Flavonoids-food sources and health benefits. *Rocz. Panstw. Zakl. Hig.* **2014**, *65*, 79–85.
32. Peluso, I.; Miglio, C.; Morabito, G.; Ioannone, F.; Serafini, M. Flavonoids and immune function in human: A systematic review. *Crit. Rev. Food Sci. Nutr.* **2015**, *55*, 383–395. [CrossRef]
33. Zeng, X.; Xi, Y.; Jiang, W. Protective roles of flavonoids and flavonoid-rich plant extracts against urolithiasis: A review. *Crit. Rev. Food Sci. Nutr.* **2019**, *59*, 2125–2135. [CrossRef]
34. Mazurakova, A.; Koklesova, L.; Samec, M.; Kudela, E.; Sivakova, J.; Pribulova, T.; Pec, M.J.; Kello, M.; Büsselberg, D.; Golubnitschaja, O.; et al. Flavonoids exert potential in the management of hypertensive disorders in pregnancy. *Pregnancy Hypertens.* **2022**, *29*, 72–85. [CrossRef] [PubMed]
35. Luo, X.; Sun, D.; Wang, S.; Luo, S.; Fu, Y.; Niu, L.; Shi, Q.; Zhang, Y. Integrating full-length transcriptomics and metabolomics reveals the regulatory mechanisms underlying yellow pigmentation in tree peony (*Paeonia suffruticosa* Andr.) flowers. *Hortic. Res.* **2021**, *8*, 235. [CrossRef]
36. Chen, C.; Zhou, G.; Chen, J.; Liu, X.; Lu, X.; Chen, H.; Tian, Y. Integrated Metabolome and Transcriptome Analysis Unveils Novel Pathway Involved in the Formation of Yellow Peel in Cucumber. *Int. J. Mol. Sci.* **2021**, *22*, 1494. [CrossRef] [PubMed]
37. Zhao, D.; Jiang, Y.; Ning, C.; Meng, J.; Lin, S.; Ding, W.; Tao, J. Transcriptome sequencing of a chimaera reveals coordinated expression of anthocyanin biosynthetic genes mediating yellow formation in herbaceous peony (*Paeonia lactiflora* Pall.). *BMC Genom.* **2014**, *15*, 689. [CrossRef]
38. Zhang, A.; Zheng, J.; Chen, X.; Shi, X.; Wang, H.; Fu, Q. Comprehensive Analysis of Transcriptome and Metabolome Reveals the Flavonoid Metabolic Pathway Is Associated with Fruit Peel Coloration of Melon. *Molecules* **2021**, *26*, 2830. [CrossRef] [PubMed]
39. Li, H.; Yang, Z.; Zeng, Q.; Wang, S.; Luo, Y.; Huang, Y.; Xin, Y.; He, N. Abnormal expression of bHLH3 disrupts a flavonoid homeostasis network, causing differences in pigment composition among mulberry fruits. *Hortic. Res.* **2020**, *7*, 83. [CrossRef]
40. Khoo, H.E.; Prasad, K.N.; Kong, K.W.; Jiang, Y.; Ismail, A. Carotenoids and their isomers: Color pigments in fruits and vegetables. *Molecules* **2011**, *16*, 1710–1738. [CrossRef]
41. Zhou, Y.; Lv, J.; Yu, Z.; Wang, Z.; Li, Y.; Li, M.; Deng, Z.; Xu, Q.; Cui, F.; Zhou, W. Integrated metabolomics and transcriptomic analysis of the flavonoid regulatory networks in Sorghum bicolor seeds. *BMC Genom.* **2022**, *23*, 619. [CrossRef]
42. Liu, J.; Zhang, X.; Tian, J.; Li, Y.; Liu, Q.; Chen, X.; Feng, F.; Yu, X.; Yang, C. Multiomics analysis reveals that peach gum colouring reflects plant defense responses against pathogenic fungi. *Food Chem.* **2022**, *383*, 132424. [CrossRef]
43. Gao, J.; Ren, R.; Wei, Y.; Jin, J.; Ahmad, S.; Lu, C.; Wu, J.; Zheng, C.; Yang, F.; Zhu, G. Comparative Metabolomic Analysis Reveals Distinct Flavonoid Biosynthesis Regulation for Leaf Color Development of Cymbidium sinense 'Red Sun'. *Int. J. Mol. Sci.* **2020**, *21*, 1869. [CrossRef]
44. Yan, H.; Pei, X.; Zhang, H.; Li, X.; Zhang, X.; Zhao, M.; Chiang, V.L.; Sederoff, R.R.; Zhao, X. MYB-Mediated Regulation of Anthocyanin Biosynthesis. *Int. J. Mol. Sci.* **2021**, *22*, 3103. [CrossRef]
45. An, J.-P.; Wang, X.-F.; Zhang, X.-W.; Xu, H.-F.; Bi, S.-Q.; You, C.-X.; Hao, Y.-J. An apple MYB transcription factor regulates cold tolerance and anthocyanin accumulation and undergoes MIEL1-mediated degradation. *Plant Biotechnol. J.* **2020**, *18*, 337–353. [CrossRef]
46. An, J.-P.; Li, H.-H.; Song, L.-Q.; Su, L.; Liu, X.; You, C.-X.; Wang, X.-F.; Hao, Y.-J. The molecular cloning and functional characterization of MdMYC2, a bHLH transcription factor in apple. *Plant Physiol. Biochem.* **2016**, *108*, 24–31, Erratum in: *Plant Physiol. Biochem.* **2019**, *135*, 612. [CrossRef]
47. Li, Y.; Xu, P.; Chen, G.; Wu, J.; Liu, Z.; Lian, H. FvbHLH9 Functions as a Positive Regulator of Anthocyanin Biosynthesis by Forming a HY5-bHLH9 Transcription Complex in Strawberry Fruits. *Plant Cell Physiol.* **2020**, *61*, 826–837. [CrossRef]
48. Huang, Y.; Vialet, S.; Guiraud, J.; Torregrosa, L.; Bertrand, Y.; Cheynier, V.; This, P.; Terrier, N. A negative MYB regulator of proanthocyanidin accumulation, identified through expression quantitative locus mapping in the grape berry. *New Phytol.* **2014**, *201*, 795–809. [CrossRef]
49. Li, M.; Sun, L.; Gu, H.; Cheng, D.; Guo, X.; Chen, R.; Wu, Z.; Jiang, J.; Fan, X.; Chen, J. Genome-wide characterization and analysis of bHLH transcription factors related to anthocyanin biosynthesis in spine grapes (*Vitis davidii*). *Sci. Rep.* **2021**, *11*, 6863. [CrossRef]
50. Kim, J.; Kim, D.H.; Lee, J.Y.; Lim, S.H. The R3-Type MYB Transcription Factor BrMYBL2.1 Negatively Regulates Anthocyanin Biosynthesis in Chinese Cabbage (*Brassica rapa* L.) by Repressing MYB-bHLH-WD40 Complex Activity. *Int. J. Mol. Sci.* **2022**, *23*, 3382. [CrossRef] [PubMed]

51. Xie, Z.; Nolan, T.M.; Jiang, H.; Yin, Y. AP2/ERF Transcription Factor Regulatory Networks in Hormone and Abiotic Stress Responses in Arabidopsis. *Front. Plant Sci.* **2019**, *10*, 228. [CrossRef] [PubMed]
52. Jiang, J.; Ma, S.; Ye, N.; Jiang, M.; Cao, J.; Zhang, J. WRKY transcription factors in plant responses to stresses. *J. Integr. Plant Biol.* **2017**, *59*, 86–101. [CrossRef] [PubMed]
53. Alabd, A.; Ahmad, M.; Zhang, X.; Gao, Y.; Peng, L.; Zhang, L.; Ni, J.; Bai, S.; Teng, Y. Light-responsive transcription factor PpWRKY44 induces anthocyanin accumulation by regulating PpMYB10 expression in pear. *Hortic. Res.* **2022**, *9*, uhac199. [CrossRef] [PubMed]
54. Chen, Y.; Wu, P.; Zhao, Q.; Tang, Y.; Chen, Y.; Li, M.; Jiang, H.; Wu, G. Overexpression of a Phosphate Starvation Response AP2/ERF Gene From Physic Nut in Arabidopsis Alters Root Morphological Traits and Phosphate Starvation-Induced Anthocyanin Accumulation. *Front. Plant Sci.* **2018**, *9*, 1186. [CrossRef]
55. He, M.; Yao, Y.; Li, Y.; Yang, M.; Li, Y.; Wu, B.; Yu, D. Comprehensive transcriptome analysis reveals genes potentially involved in isoflavone biosynthesis in *Pueraria thomsonii* Benth. *PLoS ONE* **2019**, *14*, e0217593. [CrossRef] [PubMed]
56. Zhao, Y.; Zhang, Y.-Y.; Liu, H.; Zhang, X.-S.; Ni, R.; Wang, P.-Y.; Gao, S.; Lou, H.-X.; Cheng, A.-X. Functional characterization of a liverworts bHLH transcription factor involved in the regulation of bisbibenzyls and flavonoids biosynthesis. *BMC Plant Biol.* **2019**, *19*, 497. [CrossRef]
57. Deshmukh, A.B.; Datir, S.S.; Bhonde, Y.; Kelkar, N.; Samdani, P.; Tamhane, V.A. De novo root transcriptome of a medicinally important rare tree Oroxylum indicum for characterization of the flavonoid biosynthesis pathway. *Phytochemistry* **2018**, *156*, 201–213. [CrossRef]
58. Tu, M.; Fang, J.; Zhao, R.; Liu, X.; Yin, W.; Wang, Y.; Wang, X.; Wang, X.; Fang, Y. CRISPR/Cas9-mediated mutagenesis of VvbZIP36 promotes anthocyanin accumulation in grapevine (*Vitis vinifera*). *Hortic. Res.* **2022**, *9*, uhac022. [CrossRef] [PubMed]